

# Fracture Toughness of Cu-Sn Intermetallic Thin Films

B. BALAKRISNAN,<sup>1,3</sup> C.C. CHUM,<sup>1</sup> M. LI,<sup>1</sup> Z. CHEN,<sup>2</sup> and T. CAHYADI<sup>2</sup>

<sup>1</sup>*Institute of Materials Research and Engineering, Singapore 117602.*

<sup>2</sup>*Nanyang Technological University, School of Materials Engineering,  
Singapore 639798.*

<sup>3</sup>*E-mail: b-bala@imre.org.sg*

Intermetallic compounds (IMCs) are formed as a result of interaction between solder and metallization to form joints in electronic packaging. These joints provide mechanical and electrical contacts between components. The knowledge of fracture strength of the IMCs will facilitate predicting the overall joint property, as it is more disposed to failure at the joint compared to the solder because of its brittle characteristics. The salient feature of this paper is the measurement of the fracture toughness and the critical energy-release rate of Cu<sub>3</sub>Sn and Cu<sub>6</sub>Sn<sub>5</sub> intermetallic thin films, which is the result of the interaction between Sn from the solder and Cu from the metallization. To achieve the objective, a controlled buckling test was used. A buckling test in the current work refers to one that displays large transverse displacement caused by axial compressive loading on a slender beam. The stress and strain along the beam can be easily calculated by the applied displacement. Fracture-toughness values of Cu<sub>3</sub>Sn and Cu<sub>6</sub>Sn<sub>5</sub> are 2.85 MPa√m ± 0.17 MPa√m and 2.36 MPa√m ± 0.15 MPa√m, respectively. Corresponding critical energy-release rate values are 65.5 J/m<sup>2</sup> ± 8.0 J/m<sup>2</sup> and 55.9 J/m<sup>2</sup> ± 7.3 J/m<sup>2</sup>, respectively. The values obtained were much higher than the ones measured in bulk intermetallic samples but correlated well with those values obtained from conventional fracture-toughness specimens when fracture was confined within the intermetallic layers. Hence, the controlled buckling test is a promising fast and effective way to elucidate mechanical properties of thin films.

## Keywords

Fracture toughness, critical energy-release rate, thin intermetallic films, Cu<sub>3</sub>Sn, Cu<sub>6</sub>Sn<sub>5</sub>, controlled buckling test

## INTRODUCTION

Intermetallic compounds (IMCs) are ubiquitously used in many applications because of their attractive concoction of physical and mechanical properties.<sup>1,2</sup> In the electronic-packaging industry, IMCs with several microns in thickness are found mainly in the joints as a result of interaction between solder and metallization. These joints provide mechanical and electrical contacts between the components, and the reliability of these solder joints is vital in determining the performance of the devices. Any processing defect or thermomechanical fatigue induces cracks at the solder joint, which will reduce the integrity of the device severely. Many researches in this area are focused on determining shear strength of the solder joint<sup>3-6</sup> rather than the strength of the intermetallic formed at the joint. The shear strength of a joint gives an idea about its reliability from a macroscopic viewpoint, but it is not helpful in understanding the origin of the failure from a microscopic point of view. The knowledge of the fracture strength of the intermetallic itself will help to presage the overall joint property, as it is more prone to failure at the

joint compared to the solder because of its brittle nature.

In this paper, we report the fracture toughness of  $\text{Cu}_3\text{Sn}$  and  $\text{Cu}_6\text{Sn}_5$  IMCs. The  $\text{Cu}_3\text{Sn}$  and  $\text{Cu}_6\text{Sn}_5$  thin films are the common intermetallics found in most conventional solder joints as a result of the reaction between Cu metallization and Sn from the solder. Although there have been some publications on their bulk properties,<sup>7,8</sup> not much focus has been placed on their thin-film properties. The study of mechanical properties of thin films poses a great challenge<sup>9-13</sup> because conventional mechanical-testing methods cannot be used. Incessant efforts have been placed in this area to come up with new techniques. However, no single, universally accepted methodology for measuring mechanical properties of thin films has been devised.<sup>14-19</sup>

A controlled buckling test was used to test the  $\text{Cu}_3\text{Sn}$  and  $\text{Cu}_6\text{Sn}_5$  intermetallic thin films. By measuring the critical strain necessary to initiate the first crack, the critical energy-release rates and fracture-toughness values were calculated.

## EXPERIMENTAL

### Sample Preparation

Thin metallic films of Cu and Sn were cosputtered onto polymer substrates by using a DC magnetron-sputtering machine. The total thickness of the metal film deposited was 800 nm, which is close to the thickness of the intermetallic films found in actual flip-chip packages after processing. The stoichiometric compositions were maintained during codeposition by controlling the deposition rates of individual targets. Two types of films were deposited: one with an atomic ratio of Cu to Sn of 3:1 on a polyetherimide (Ultem) substrate and another with 6:5 on a polycarbonate (PC) substrate, and they were referred to as sample A and B, respectively. The sputtering conditions and substrates properties are given in Table I. Both types of samples were annealed in inert  $\text{N}_2$  ambience for a day. The aim of annealing was to ensure complete formation of the desired intermetallic phases and to reduce any residual stresses in the film. Sample A was annealed at  $150^\circ\text{C}$  to form the  $\text{Cu}_3\text{Sn}$  IMC. Sample B was annealed at a lower temperature of  $50^\circ\text{C}$  to form  $\text{Cu}_6\text{Sn}_5$  and to avoid the conversion of this phase to  $\text{Cu}_3\text{Sn}$ .<sup>20</sup> Ultem substrates rather than PC substrates were used for  $\text{Cu}_3\text{Sn}$ , as the annealing temperature used is higher than the stability temperature of PC.

The annealed films were characterized using a scanning electron microscope (SEM) equipped with energy dispersive spectroscopy (EDS) for microstructure and compositional analysis and using x-ray diffraction (XRD) for phase identification. To check the adhesion between the film and the polymer substrate, a simple scotch-tape test was used. During this test, commercially available adhesive tape was applied on the film top surface and then was peeled off slowly. The peeled surface was examined for signs of delamination or complete removal of the film from which a qualitative assessment of the adhesion was obtained.

### Specimen Geometry and Experimental Procedure

Beam specimens were used for the controlled buckling test. The dimensions of the samples were  $48\text{ mm} \times 3\text{ mm} \times 0.175\text{ mm}$  for sample A and  $48\text{ mm} \times 3\text{ mm} \times 0.5\text{ mm}$  for sample B. The ratio of the thickness of the IMC to the thickness of the substrate was very small (1:200 for sample A and 1:600 for sample B). Figure 1 shows the experimental

setup for the controlled buckling test, which consists of a jig having two clamps, where one end is fixed, while the other end is movable. The jig is secured onto a measuring optical-microscope stage. The sample is clamped between the two ends, and the distance between the two ends is 35 mm. Force is applied gradually by moving the spindle of the micrometer, which, in turn, buckles the sample. Simultaneously, the center region of the specimen was monitored for crack initiation by using a measuring optical microscope. Gradual spindle movement and careful monitoring are very crucial to see the first channeling-crack formation. Time taken between each spindle movement was approximately kept constant, about 45 sec. Around eight to nine samples were tested for each type of intermetallic.

## RESULTS AND DISCUSSION

### Characterization of Samples

Annealed sample A appeared smooth and shiny with a surface roughness around 5 nm. While annealed sample B appeared dull and whitish in color with a surface roughness around 60 nm. Annealing did not affect the physical appearance of the films formed. Figure 2 shows SEM micrographs of sample A and B after annealing for a day at 150°C and 50°C, respectively. The micrographs show that the films were continuous with grain size around 100 nm for sample A, and as for sample B, the grain sizes ranged between 200 nm and 400 nm. For sample B, large grains and small grains occur concurrently. The EDS was used to check the atomic ratio of Cu to Sn in the films; for sample A, the ratio was about 3:1, and for sample B, the ratio was about 6:5. These atomic ratios correspond to the Cu<sub>3</sub>Sn (sample A) and Cu<sub>6</sub>Sn<sub>5</sub> (sample B) phases, which were further confirmed by XRD. Figure 3 shows the XRD spectra obtained for sample A and sample B. Six distinctive peaks at 37.5°, 41.9°, 43.2°, 57.5°, 67.8°, and 77.4° for sample A conform well with the (0 16 0), (0 0 2), (2 12 0), (0 16 2), (0 8 3), and (2 26 1) planes of Cu<sub>3</sub>Sn. Similarly, the peaks at 29.9°, 42.7°, 43.6°, 53.1°, 62.4°, 70.6°, and 78.6° for sample B conform well with the (2 2 1), (1 3 2), (4 2 2), (2 4 1), (4 2 2), (3 5 1), and (0 6 0) planes of Cu<sub>6</sub>Sn<sub>5</sub>. These results show that sample A is Cu<sub>3</sub>Sn, whereas sample B is Cu<sub>6</sub>Sn<sub>5</sub>.

### Residual Stress Measurement

Sputtered film generally exhibits residual stress. The residual stress in the film needs to be either subtracted or added to the externally applied stress to obtain the true stress in film at crack initiation.

Average biaxial-residual stress in the film,  $\sigma_f$ , can be calculated using the following equation:<sup>21</sup>

$$\sigma_f = \left\{ \frac{E_s h^2 \kappa}{6(1 - \nu_s) h_f} \right\} \left\{ \frac{1 + \sum \xi^3}{1 + \xi} \right\} \quad (1)$$

$$\text{where } \xi = \frac{h_f}{h_s}; \quad \Sigma = \frac{E_f/1 - \nu_f}{E_s/1 - \nu_s} \quad (2)$$

The terms E, h,  $\kappa$ , and  $\nu$  represent Young's modulus, thickness, bending curvature, and Poisson's ratio, respectively. The subscript s is used to denote the substrate, and f is for the thin intermetallic film. By using the preceding equations, Cu<sub>3</sub>Sn film on the Ultem

substrate was found to exhibit a residual compressive stress of 70 MPa even after annealing for 1 day. However, Cu<sub>6</sub>Sn<sub>5</sub> on PC did not exhibit noticeable residual stress.

### Fracture-Toughness Measurement

The crack was always found to initiate at the edges of the sample. The extension,  $e_c$ , at which the crack initiates, is used to compute the critical energy-release rate,  $G_c$ .<sup>22</sup> A large deflection-theory solution for clamped ends is used to express the radius of curvature,  $R$ , in terms of  $e_c$ .<sup>23</sup> Figure 4 shows a schematic diagram of the cross section of the buckled sample.

$$\frac{L}{R} = NkK(k) \quad (3)$$

$$\frac{e_c}{L} = 2 \left[ 1 - \frac{E(k)}{K(k)} \right] \quad (4)$$

where  $L$  is the length of the film (distance between the clamped ends), which is around 35 mm;  $K(k)$  and  $E(k)$  are complete elliptic integrals of the first and second kind; and  $N$  is 8 for clamped ends.

Hence, from  $R$ , the critical strain,  $\epsilon_c$ , can be obtained using this formula:

$$\epsilon_c = \frac{h_s}{2R} \quad (5)$$

Because the film thickness is very small compared to the thickness of the polymer substrate used in the experiment, the neutral axis is taken as the center of the substrate. All the extension values that were obtained from observing the onset of crack initiation from the experiments carried out on the controlled buckling test are converted into strain values. These strain values obtained for Cu<sub>6</sub>Sn<sub>5</sub> and Cu<sub>3</sub>Sn thin-intermetallic films are tabulated in Tables II and III, respectively. Corresponding stress values are also tabulated for comparison. The Young's modulus of Cu<sub>3</sub>Sn and Cu<sub>6</sub>Sn<sub>5</sub> were taken as 110 GPa and 90 GPa, respectively, for the stress calculation.<sup>24</sup>

From the critical strain value, critical energy-release rate,  $G_c$ , is calculated as

$$G_c = \frac{1}{2}[\epsilon_c^2 \bar{E}_f g(\alpha, \beta) h_f] \quad (6)$$

$$\alpha = \frac{\bar{E}_f - \bar{E}_s}{\bar{E}_f + \bar{E}_s}; \beta = \frac{\bar{E}_f \left( \frac{1 - 2\nu_s}{1 - \nu_s} \right) - \bar{E}_s \left( \frac{1 - 2\nu_f}{1 - \nu_f} \right)}{2(\bar{E}_f + \bar{E}_s)} \quad (7)$$

The  $\bar{E}$  term denotes the plain strain-elastic moduli, and  $g(\alpha, \beta)$  is a function of the two Dundurs parameters  $\alpha$  and  $\beta$ .<sup>21,25,26</sup> The more important of these two parameters is  $\alpha$ , which is a measure of the mismatch in the moduli between the intermetallic film and the polymer substrate. The value of  $\alpha$  can vary from  $-1$  for a rigid substrate to  $1$  for an infinitely compliant substrate. For Cu<sub>3</sub>Sn on the Ultem substrate,  $\alpha = 0.9523$ , and for Cu<sub>6</sub>Sn<sub>5</sub> on the PC substrate,  $\alpha = 0.9523$ .

Table II shows the  $G_c$  values obtained for  $\text{Cu}_6\text{Sn}_5$  for the corresponding strain values. The average critical energy-release rate was found to be  $55.9 \text{ J/m}^2 \pm 7.3 \text{ J/m}^2$ . This corresponds to a fracture-toughness value ( $K_{IC}$ ) of  $2.36 \text{ MPa}\sqrt{\text{m}} \pm 0.15 \text{ MPa}\sqrt{\text{m}}$

The critical energy-release rate for  $\text{Cu}_3\text{Sn}$  is calculated from critical strain after correcting for finite residual stress. The true strain and critical energy-release rate computed for  $\text{Cu}_3\text{Sn}$  values are tabulated in Table III. The average critical energy-release rate was found to be  $65.5 \text{ J/m}^2 \pm 8 \text{ J/m}^2$ . This corresponds to a fracture-toughness value ( $K_{IC}$ ) of  $2.85 \text{ MPa}\sqrt{\text{m}} \pm 0.17 \text{ MPa}\sqrt{\text{m}}$ .

Cracks that initiated at the edge of the sample gradually propagated the full width of the sample. Further application of the force increases the intensity of the cracks. Figure 5a shows a typical optical micrograph of the cracks seen in the  $\text{Cu}_3\text{Sn}$  film that was taken after the full propagation of the cracks. No delamination of the intermetallic film from the substrate was observed, indicating a good adhesion between film and substrate. Figure 5b shows a crack formed on  $\text{Cu}_6\text{Sn}_5$  at high magnification. Intergranular crack propagation was observed.

Table IV shows the fracture-toughness values obtained from the literature for the Cu-Sn samples. The work of Fields et al.<sup>7</sup> used bulk samples, and the technique used was indentation. The values obtained in our experiment were twice as much as obtained by Fields et al. This is plausible because it is a generally acknowledged fact that the fracture-toughness values of thin films are expected to be higher than that of their corresponding bulk samples. This happens because, in the bulk samples, the number of sites for crack initiation is much higher than in thin films. Frear and Vianco<sup>28</sup> used bulk Cu, half compact-tension specimens joined together by 0.254-mm-thick solders along the crack propagation path. They found that the failure mode was through the solders for as-reflowed samples when the intermetallics were thin. After annealing, the intermetallics became thicker, and the failure modes shifted toward intermetallics fracture or fracture at the interface between solders and intermetallics. The toughness for the solder fracture was reported to be  $4 \text{ MPa}\sqrt{\text{m}} \pm 0.5 \text{ MPa}\sqrt{\text{m}}$ . This low value was due to the high constraint to solder deformation by the bulk Cu specimens. Failure through  $\text{Cu}_6\text{Sn}_5$  was found to correspond to bulk-specimen fracture toughness between  $2 \text{ MPa}\sqrt{\text{m}}$  and  $6 \text{ MPa}\sqrt{\text{m}}$ . There was no report on the fracture toughness of  $\text{Cu}_3\text{Sn}$  by Frear and Vianco,<sup>28</sup> although crack propagation through  $\text{Cu}_3\text{Sn}$  was also observed. The authors did not give an explanation for the large disparity in toughness values of  $\text{Cu}_6\text{Sn}_5$ . In their work, it was very difficult or almost impossible to identify the crack initiation sites given the complexity of the microstructures at the interface. It was possible that a main crack initiated elsewhere and propagated into the intermetallic layers. Therefore, the  $K_{IC}$  of  $2\text{--}6 \text{ MPa}\sqrt{\text{m}}$  may only serve as an indication of the range of fracture toughness for the intermetallics. Our results are well within the range suggested by Frear and Vianco.<sup>28</sup> The advantage of the current study is that the measurement was carried out in the prepared single-phase thin-film IMCs; therefore, ambiguity was eliminated. Another uniqueness is that the disparity in toughness values is very low, which would reinforce the credibility of the results.

Pratt and Quesnel<sup>28</sup> demonstrated the importance of the intermetallic joint strength in determining the overall integrity of the system. Their study showed how the fracture toughness of bulk solder, which was  $70 \text{ MPa}\sqrt{\text{m}}$ , decreased to  $3 \text{ MPa}\sqrt{\text{m}}$  because of the constraint of the joint in the assembly. Thus, our finding on the fracture toughness of the thin intermetallic films will be valuable in predicting the reliability of the solder joint.

These values will be vital for modeling the devices.

In summary, using the technique of controlled buckling test, the important mechanical property of fracture toughness can readily be measured.

## **CONCLUSIONS**

The critical energy release-rate of intermetallic thin films, namely,  $\text{Cu}_3\text{Sn}$  and  $\text{Cu}_6\text{Sn}_5$ , were measured using the controlled buckling test. This is a fast and effective way of measuring the critical energy-release rate or fracture toughness of thin intermetallic film. Proper control of the sample preparation condition and careful observation of the crack-initiation point measurement are vital in determining an accurate value. The  $G_c$  values obtained through the experiment are  $65.5 \text{ J/m}^2$  and  $55.9 \text{ J/m}^2$  for  $\text{Cu}_3\text{Sn}$  and  $\text{Cu}_6\text{Sn}_5$ , respectively. The corresponding fracture-toughness values are  $2.85 \text{ MPa}\sqrt{\text{m}}$  and  $2.36 \text{ MPa}\sqrt{\text{m}}$  for  $\text{Cu}_3\text{Sn}$  and  $\text{Cu}_6\text{Sn}_5$ , respectively. Using these values instead of bulk values to predict the solder-joint property would be an effective way to predict any premature failure.

## **ACKNOWLEDGEMENTS**

The authors thank Dr. Brian Cotterell for his advice and Miss Shen Lu and Mr. TohKee Chua for their technical assistance.

## REFERENCES

- [1] N.S. Stoloff, C.T. Liu, and S.C. Deevi, *Intermetallics*8, 1313 (2000).
- [2] R.W. Cahn, *Intermetallics* 6, 563 (1998).
- [3] J.K. Kim, M.S. Suk, and H.Y. Kwon, *Surf. Coating Technol.* 82, 23 (1996).
- [4] R.E. Pratt, E.I. Stromwold, and D.J. Quesnal, *J. Electron. Mater.* 23, 375 (1994).
- [5] J. Sigelko, S. Choi, K.N. Subramanian, J.P. Lucas, and T.R. Bieler, *J. Electron. Mater.* 28, 1184 (1999).
- [6] Y.C. Chan, A.C.K. So, and J.K.L. Lai, *Mater. Sci. Eng. B* 55, 5 (1998).
- [7] R.J. Fields, S.R. Low III, and G.K. Lucey, Jr., *The Metal Science of Joining*, ed. M.J. Cieslak, J.H. Perepezko, S. Kang, and M.E. Glicksman (Warrendale PA: TMS, 1992), pp. 165–173.
- [8] K. Nakajima, A. Isogai, and Y. Taga, *Jpn. J. Appl. Phys. Suppl.* 2, 309 (1974).
- [9] R.P. Vinci and J.J. Vlassak, *Ann. Rev. Mater. Sci.* 26, 432 (1996).
- [10] D.S. Campbell, *Handbook of Thin Film Technology*, ed. L.I. Maissel and R. Glang (New York: McGraw-Hill, 1971).
- [11] A.J. Griffin, F.R. Brotzen, and C.F. Dunn, *Thin Solid Films* 220, 265 (1992).
- [12] F.R. Brotzen, *Int. Mater. Rev.* 39, 24 (1994).
- [13] K. Hashimoto, M. Sakane, M. Ohnami, and T. Yoshida, *J. Soc. Mater. Sci. Jpn.* 43, 703 (1994).
- [14] W.N. Sharpe, Jr., B. Yuan, and R.L. Edwards, *J. Micromech. Sys.* 6, 193 (1997).
- [15] O.R. Shojaei and A. Karimi, *Thin Solid Films* 332, 202 (1998).
- [16] L. Gan, B.B. Nissan, and A.B. David, *Thin Solid Films* 290, 362 (1996).
- [17] V. Navratil and V. Stejskalova, *Phys. Status Solidi*, A157, 345 (1996).
- [18] W.D. Nix, *Mater. Sci. Eng.* A234, 37 (1997).
- [19] S. Makarov, E. Chilla, and H.J. Frohlich, *IEEE1995, Ultrasonics Symp. Proc.* (Piscataway, NJ: IEEE, 1995), pp. 357–360.
- [20] K.N. Tu, *Mater. Chem. Phys.* 46, 217 (1996).
- [21] J.W. Hutchinson, *Mechanics of Thin Films and Multi-layers*(Lyngby, Denmark:

Technical University of Denmark, 1996).

- [22] Z. Chen, B. Cotterell, W. Wang, E. Guenther, and S.J. Chua, *Thin Solid Films* 394, 202 (2001).
- [23] S.J. Britvec, *The Stability of Elastic Systems* (New York: Pergamon Press, 1973).
- [24] J.H. Westbrook and R.L. Fleischer, eds., *Structural Applications of Intermetallic Compounds* (New York: Wiley, 2000).
- [25] B. Cotterell and Z. Chen, *Int. J. Fract.* 104, 169 (2000).
- [26] J.W. Hutchinson and Z. Suo, *Adv. Appl. Mech.* 29, 63 (1992).
- [27] K.S. Siow and M. Manoharan, Proc. 1st IPC/SMTA *Electronics Assembly Expo* (Providence, RI: Institute PC and Surface Mount Technology Association, 1998), pp. S19-3-1– S19-3-8.
- [28] D.R. Frear and P.T. Vianco, *Metall. Mater. Trans.* A 25A, 1509 (1994).
- [29] R.E. Pratt and D.J. Quesnel, *The Metal Science of Joining*, ed. M.J. Cielak, J.H. Perepezko, and M.E. Glicksman (Warrendale, PA: TMS, 1992), pp. 201–210.

## List of Tables

Table. 1 Properties of the Films, Substrate, and Processing Condition Used

Table. 2 Experimental Results for  $\text{Cu}_6\text{Sn}_5$

Table. 3 Experimental Results for  $\text{Cu}_3\text{Sn}$

Table. 4 Comparison of Fracture Toughness of Bulk and Thin Films of  $\text{Cu}_3\text{Sn}$  and  $\text{Cu}_6\text{Sn}_5$

## List of Figures

- Figure. 1 The experimental setup of the test jig: (a) photo and (b) schematic cross-sectional diagram.
- Figure. 2 The SEM micrograph of (a) sample A and (b) sample B annealed at 150°C and 50°C, respectively.
- Figure. 3 The XRD spectrum of sample A and sample B.
- Figure. 4 The schematic diagram of the cross section of the buckled sample.
- Figure. 5 The images of the film after controlled buckling test: (a) cracks observed under the optical microscope on  $\text{Cu}_3\text{Sn}$  film and (b) the SEM image of the cracks formed on  $\text{Cu}_6\text{Sn}_5$  showing intergranular cracking.

**Table I. Properties of the Film, Substrate, and Processing Condition Used**

	<b>Sample A</b>	<b>Sample B</b>
<b>Film</b>		
Sputtering power Cu:Sn	100:140 W	160:120 W
Atomic ratio of Cu:Sn	3:1	6:5
Thickness	800 nm	800 nm
Intended intermetallic	Cu <sub>3</sub> Sn	Cu <sub>6</sub> Sn <sub>5</sub>
<b>Substrate</b>		
Type	Polyetherimide (Ultem)	Polycarbonate
Dimension	48 mm × 3 mm × 0.175 mm	48 mm × 3 mm × 0.5 mm
Glass-transition temperature	247°C	145°C
Young's modulus	2.6 GPa	2.3 GPa
Poisson's ratio	0.36	0.36
<b>Processing Condition</b>		
Annealing temperature	150°C	50°C
Annealing time	1 day	1 day

Table 1

<b>Table II. Experimental Results for Cu<sub>6</sub>Sn<sub>5</sub></b>			
<b>Number</b>	<b>Strain (%)</b>	<b>Stress (GPa)</b>	<b>G<sub>c</sub> (J/m<sup>2</sup>)</b>
1	0.702	0.704	51.05
2	0.698	0.699	50.34
3	0.807	0.809	67.37
4	0.772	0.774	61.72
5	0.726	0.728	54.51
6	0.769	0.771	61.21
7	0.706	0.708	51.57
8	0.654	0.656	44.32
9	0.767	0.769	60.82

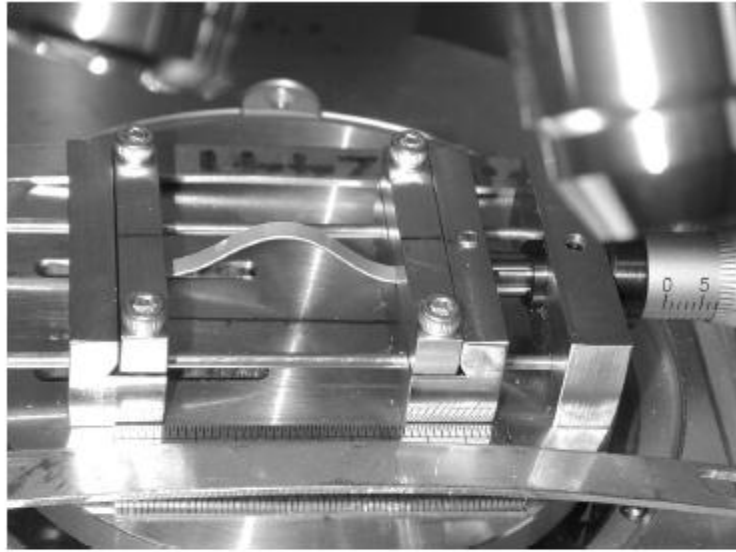
Table 2

Table III. Experimental Results for Cu <sub>3</sub> Sn					
Number	Total Strain (%)	Total Stress (GPa)	True Stress (GPa)	True Strain (%)	Gc (J/m <sup>2</sup> )
1	0.692	0.848	0.809	0.660	59.75
2	0.730	0.895	0.856	0.698	66.88
3	0.788	0.966	0.927	0.756	78.47
4	0.770	0.944	0.905	0.738	74.80
5	0.688	0.843	0.804	0.656	59.06
6	0.739	0.906	0.867	0.707	68.67
7	0.684	0.839	0.800	0.652	58.40
8	0.682	0.836	0.797	0.650	58.02

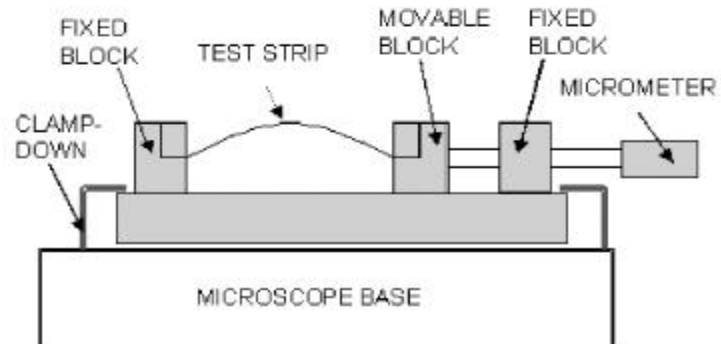
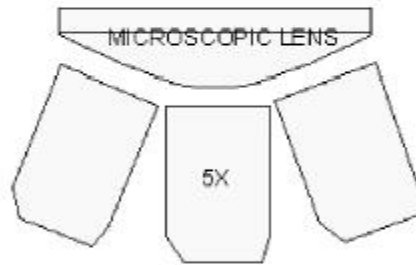
Table 3

Intermetallic Compounds	Sample Type	Fracture Toughness ( $\text{MPa}\sqrt{\text{m}}$ )	Remarks
$\text{Cu}_3\text{Sn}$	Bulk IMC	$1.7 \pm 0.3$	Indentation <sup>7</sup>
	No details	2	Other work cited in Ref. 27
$\text{Cu}_6\text{Sn}_5$	Thin film IMC	$2.85 \pm 0.17$	Current study
	Bulk IMC	$1.4 \pm 0.3$	Indentation <sup>7</sup>
	Constrained solder	2-6	Compact tension <sup>28</sup>
	Thin IMC	$2.36 \pm 0.15$	Current study

Table 4

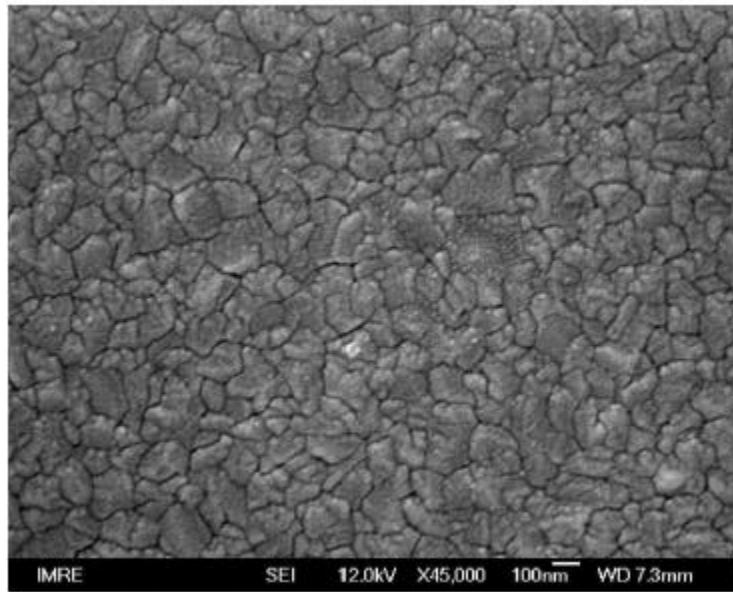


a

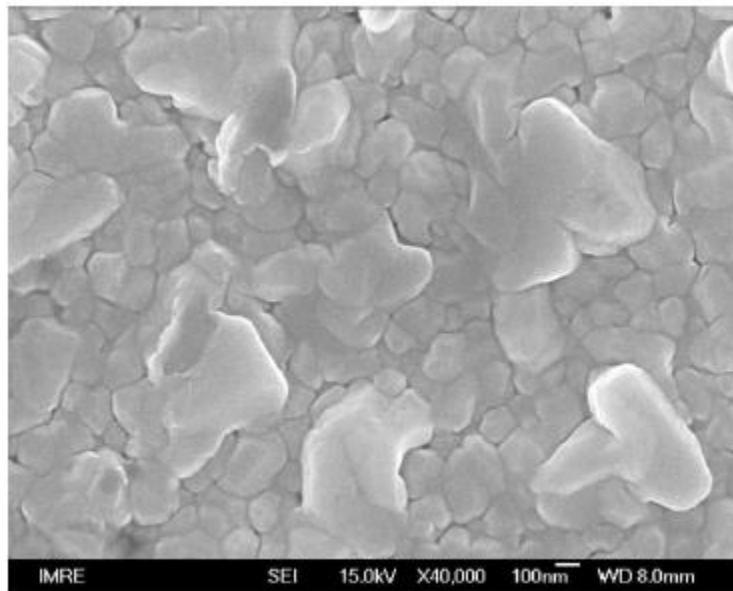


b

Figure 1



a



b

Figure 2

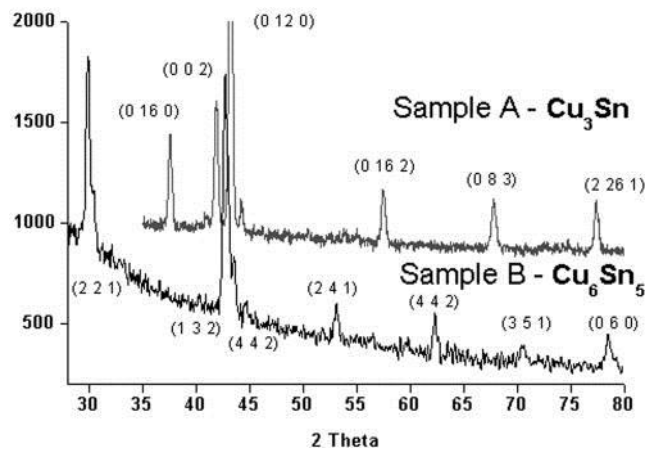


Figure 3

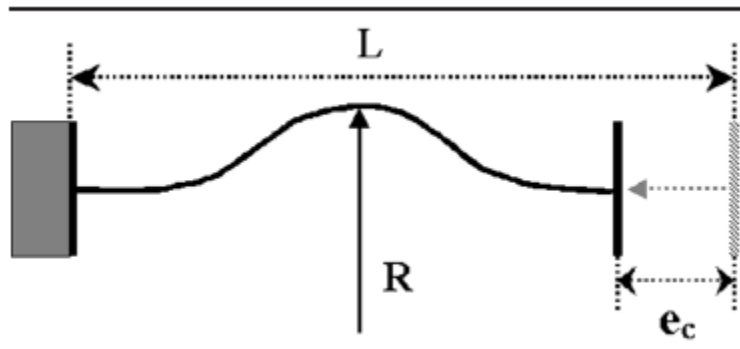
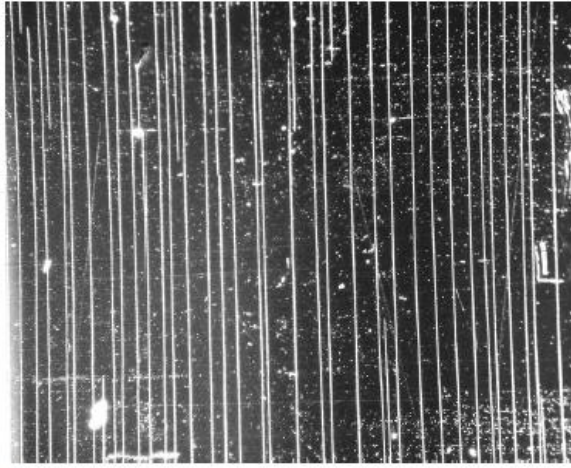
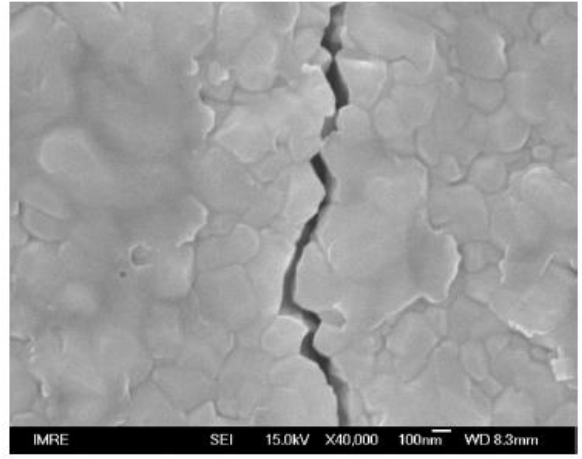


Figure 4



a



b

Figure 5